

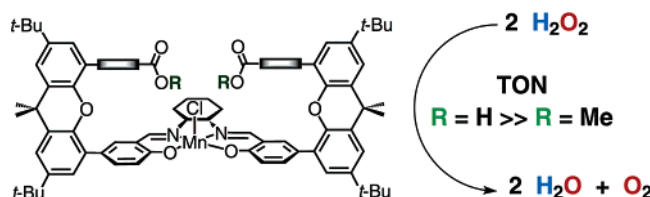
Hangman Salen Platforms Containing Two Xanthene Scaffolds

Jenny Y. Yang, Julien Bachmann, and Daniel G. Nocera*

Department of Chemistry, 6-335, Massachusetts Institute of Technology, 77 Massachusetts Avenue,
Cambridge, Massachusetts 02139-4301

nocera@mit.edu

Received June 25, 2006



A synthetic strategy for the construction of chiral salen ligands bearing two rigid xanthene spacers functionalized with carboxylic acid and ester groups is presented. Suzuki cross-coupling methodology is used to furnish the appropriately functionalized xanthene spacers to a salicylaldehyde, which is subsequently condensed with (1*R*,2*R*)-(–)-1,2-diaminocyclohexane to produce salen ligands featuring an expandable molecular cleft capable of multiple hydrogen-bonding interactions in addition to metallosalen oxidation chemistry. The ability of these “Hangman” platforms to support multielectron chemistry mediated by proton-coupled electron transfer (PCET) is established by their proclivity to promote the catalytic disproportionation of hydrogen peroxide to oxygen and water via a high-valent metal oxo. Within this functionalized Hangman framework, the stereochemistry of the cyclohexyl backbone of the salen platform is revealed in the epoxidation of 1,2-dihydronaphthalene by the metal oxo.

Introduction

Small molecule catalysis involving the making and breaking of substrate bonds in nature is often coupled to the transport of both protons and electrons.^{1–4} Our interest in catalytic processes that are driven by proton-coupled electron transfer (PCET) has led us to design “Hangman” ligand constructs, which position an acid–base functionality over the face of a redox cofactor.^{5–8} In these systems, the acid–base functional group controls the secondary coordination sphere for substrate assembly and activation by the proton. In porphyrin Hangman platforms, the high-valent metal oxo heme, evocative of the catalytic cofactor of mono-oxygenases, is unmasked by shuttling a proton from

the hanging acid–base group to a peroxide ligated to the metalloporphyrin.^{1,5–7} Our interest in generalizing the Hangman approach led us to replace metal porphyrins with Schiff base macrocycles.⁸ The synthesis of the HSX platform (pictured in Chart 1) allows for the electronic and steric properties of the redox platform to be more easily tuned than porphyrins. In addition, the chiral framework that has been the centerpiece of the development of metal salens as asymmetric oxidation catalysts^{9,10} can be installed into a salen platform, though not specifically for HSX since the acid-functionalized xanthene is bound to a salophen ligand through the phenylenediamine bridge.⁸ To rectify this design flaw, we describe the synthesis of the HSX* and H_{ph}SX* ligands shown in Chart 1. The rigid hydrogen bond functionalities are poised over a salen platform that incorporates a chiral cyclohexanediiimine bridge. To accommodate the aliphatic bridge, we have modified the attachment point of the functionalized xanthene spacer to the phenolic arms of the ligand. The incorporation of two xanthene scaffolds forms a convergent and symmetric molecular cleft of two different sizes formed from a hydrogen bond group directly attached to the xanthene and via a phenylene spacer. The PCET

(1) Chang, C. J.; Chang, M. C. Y.; Damrauer, N. H.; Nocera, D. G. *Biophys. Biochim. Acta* **2004**, *1655*, 13–28.

(2) Stubbe, J.; Nocera, D. G.; Yee, C. S.; Chang, M. C. Y. *Chem. Rev.* **2003**, *103*, 2167–2202.

(3) Cukier, R. I.; Nocera, D. G. *Annu. Rev. Phys. Chem.* **1998**, *49*, 337–369.

(4) Dempsey, J. L.; Esswein, A. J.; Manke, D. R.; Rosenthal, J.; Soper, J. D.; Nocera, D. G. *Inorg. Chem.* **2005**, *44*, 6879–6892.

(5) Yeh, C.-Y.; Chang, C. J.; Nocera, D. G. *J. Am. Chem. Soc.* **2001**, *5*, 1513–1514.

(6) Chng, L. L.; Chang, C. J.; Nocera, D. G. *Org. Lett.* **2003**, *5*, 2421–2424.

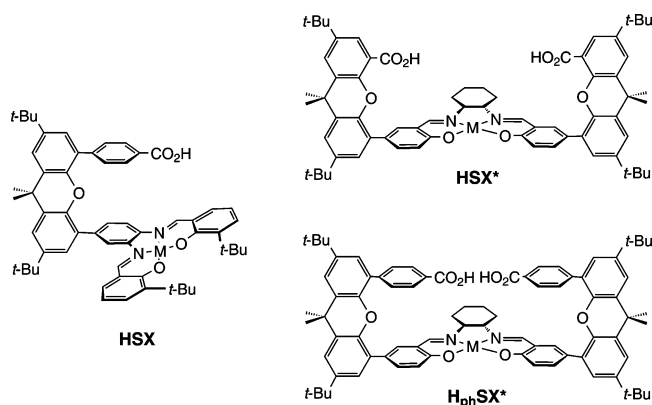
(7) Chang, C. J.; Chng, L. L.; Nocera, D. G. *J. Am. Chem. Soc.* **2003**, *125*, 1866–1876.

(8) Liu, S.-Y.; Nocera, D. G. *J. Am. Chem. Soc.* **2005**, *127*, 5278–5279.

(9) Zhang, W.; Loebach, J. L.; Wilson, D. R.; Jacobsen, E. N. *J. Am. Chem. Soc.* **1990**, *112*, 2081–2083.

(10) Irie, R.; Noda, K.; Ito, Y.; Matsumoto, N.; Katsuki, T. *Tetrahedron Lett.* **1990**, *31*, 7345–7348.

CHART 1



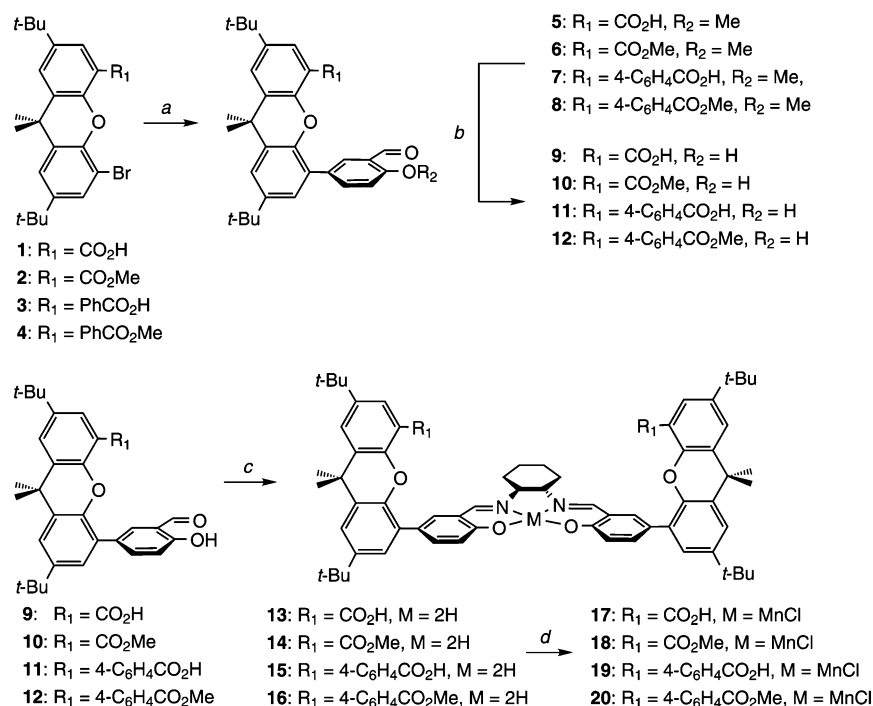
catalysis of the HSX* and H_{ph}SX* platforms has been evaluated by examining their catalase and epoxidation activity. We show that the benefits of the hanging group for substrate assembly over the redox active metal center are preserved, while this architecture permits the additional feature of enantioselective activity.

Results and Discussion

Initial attempts to synthesize **9**, which is the precursor to HSX*, followed established methods to functionalize the xanthene bridge selectively with a carboxylic acid (**1**) from the commercially available xanthene dibromide (see Scheme S1, in the Supporting Information).⁷ The methyl ester (**2**) derivative is obtained directly by protection of **1**.⁷ We initially focused on obtaining **9** by replacing the bromide in **1** with a boronic acid in order to establish a site for subsequent cross-coupling with 5-bromosalicylaldehyde. This was achieved using palladium-catalyzed cross-coupling conditions with bis(pinacolato)diboron,

but only after protection of the acid with an ester.¹¹ Methyl ester **2** was used to obtain boronic acid precursor **24**, which was then coupled to 5-bromosalicylaldehyde to afford precursor **10**; the methyl ester serves as the protecting group.^{12,13} The two coupling steps provided product in moderate yields, but the methyl ester proved difficult to deprotect. Using a benzyl ester protecting group on the acid¹⁴ to make **25**, and following the same synthetic route also resulted in a modest yield in the successive palladium-catalyzed cross-coupling steps. As a result, although the benzyl ester was easier to cleave, the overall yield along this synthetic pathway was not favorable. We therefore sought an alternative synthetic pathway to the Hangman salens.

Scheme 1 outlines the synthetic strategy that successfully delivers the HSX* and H_{ph}SX* ligands in good yields. The stepwise functionalization of the commercially available xanthene dibromide furnishes the benzoic acid methyl ester⁸ (**4**), which can be deprotected to give the benzoic acid analogue (**3**). With the appropriately functionalized xanthene precursors (**1–4**) in hand, the construction of the salen macrocycle begins with the catenation of 3-formyl-4-methoxyphenyl boronic acid to the remaining bromide of **1–4**. Effectively the site of boronic acid and bromide functionalization on the xanthene and salicylaldehyde has been inverted from that of Scheme S1. We found that this modification provided a better nucleophilic site for the Suzuki cross-coupling step than of the boronic acid functionalized xanthene and consequently delivered **5–8** in good yields.¹⁵ Subsequent deprotection of the methyl ether by treatment with boron tribromide yields the appropriate xanthene-functionalized salicylaldehyde derivatives **9–12**.^{16,17} Boron tribromide is also known to deprotect methyl esters;¹⁸ however, **10** and **12** can be isolated by reducing the reaction time to selectively cleave the methyl ether to achieve the desired product. The construction of the salen ring is completed with the condensation, in high yield, of **9–12** with 0.5 equiv of

SCHEME 1 ^a

^a Reagents: (a) 3-Formyl-4-methoxyphenylboronic acid, Na₂CO₃, Pd(PPh₃)₄, DMF/H₂O; (b) BBr₃, CH₂Cl₂; (c) (1*R*,2*R*)-(–)-1,2-diaminocyclohexane, EtOH; (d) (i) Mn(OAc)₂(H₂O)₄, EtOH, (ii) aq NaCl.

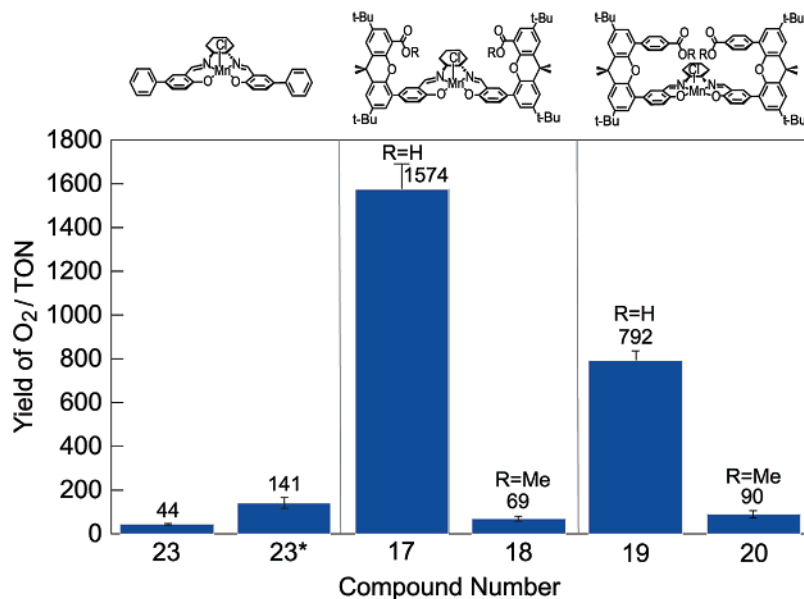


FIGURE 1. Turnover number (TON) of hydrogen peroxide dismutation catalyzed by manganese compounds **23** (**23*** in the presence of 2 equiv of benzoic acid), **17**, **18**, **19**, and **20** after 1 h.

(1*R*,2*R*)-(–)-1,2-diaminocyclohexane to produce the desired Hangman salen ligands **13**–**16**. Mass spectral evidence shows no evidence of any singly condensed diamine product, and the ¹H NMR integrations are consistent with two functionalized xanthenes to one cyclohexyldiamine bridge. Analogous porphyrins ligands bearing two xanthene bridges possess two different atropisomers (xanthenes facing each other across the macrocycle as opposed to the xanthenes being one-up and one-down) that can be independently identified by ¹H NMR spectroscopy. For these porphyrin ligands, no exchange is observed between the two atropisomers in solution at room temperature.^{15,19} In contrast, the ¹H NMR for the HSX* and H_{ph}SX* ligands at room temperature show only one set of well-resolved ligand peaks, suggesting there is either one atropisomer in solution or exchange between the two is extremely rapid. Manganese ion may be inserted into the salen core by refluxing the ligand with an excess of manganese acetate in air, followed by workup with a saturated aqueous sodium chloride solution. Products **17**–**20** are obtained with chloride ion occupying an axial coordination position of the Mn(III) ion.

Complexes **17** and **19** comprise a structurally homologous series of doubly bridged Hangman constructs in which the acid–base group can be differentially extended over the face of the salen. Since the metal ion defines the site for substrate binding and activation, the positioning of the acid–base group proximal

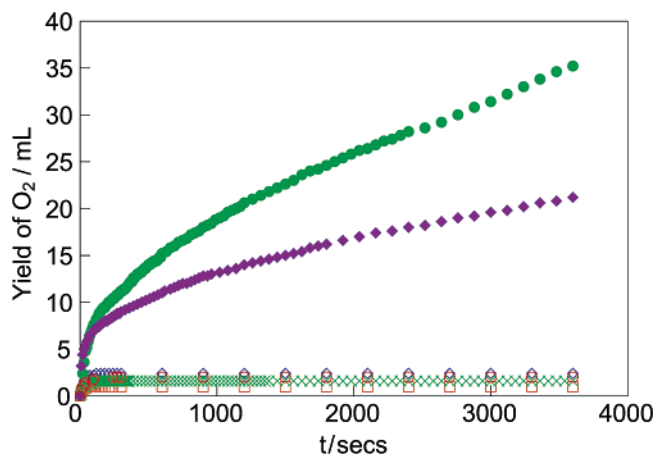


FIGURE 2. Oxygen release from hydrogen peroxide dismutation catalyzed by manganese compounds **23** (□), **23*** (*in the presence of 2 equiv of benzoic acid) (◇), **17** (●), **18** (×), **19** (◆), and **20** (○) over 1 h.

to the metal, a priori, would appear to be important to the PCET activity of these doubly bridged Hangman salens. To probe this issue, the PCET activation of O–O bonds by **17** and **19** was examined by studying the disproportionation of H₂O₂, an important PCET process that is catalyzed by a variety of enzymes.²⁰ Figure 1 shows the turnover numbers (TONs) for oxygen production by **17** and **19** and control systems in which (i) a proton is absent from the hanging group (**18** and **20**) and (ii) the salen platform is unmodified [Mn(5-phsalen)Cl] (**23**). The presence of the acid–base hanging group results in a dramatic increase in catalase-type reactivity. Whereas high TONs can be achieved with **17** and **19**, relatively low TONs are observed when the carboxylic acid functionality is replaced by an ester (**18** and **20**). Similarly, control experiments with the redox-only manganese salen complex **23** show low activity for disproportionation. The addition of an external H⁺ source

(11) Ishiyama, T.; Murata, M.; Miyaura, N. *J. Org. Chem.* **1995**, *60*, 7508–7510.

(12) Deng, Y.; Chang, C. K.; Nocera, D. G. *Angew. Chem., Int. Ed.* **2000**, *39*, 1066–1068.

(13) Miyaura, N.; Suzuki, A. *Chem. Rev.* **1995**, *95*, 2457–2483.

(14) Neises, B.; Andries, T.; Steglich, W. *J. Chem. Soc., Chem. Commun.* **1982**, 1132–1133.

(15) Chang, C. J.; Yeh, C.-Y.; Nocera, D. G. *J. Org. Chem.* **2002**, *67*, 1403–1406.

(16) Kende, A. S.; Rizzi, J. P. *Tetrahedron Lett.* **1981**, *22*, 1779–1982.

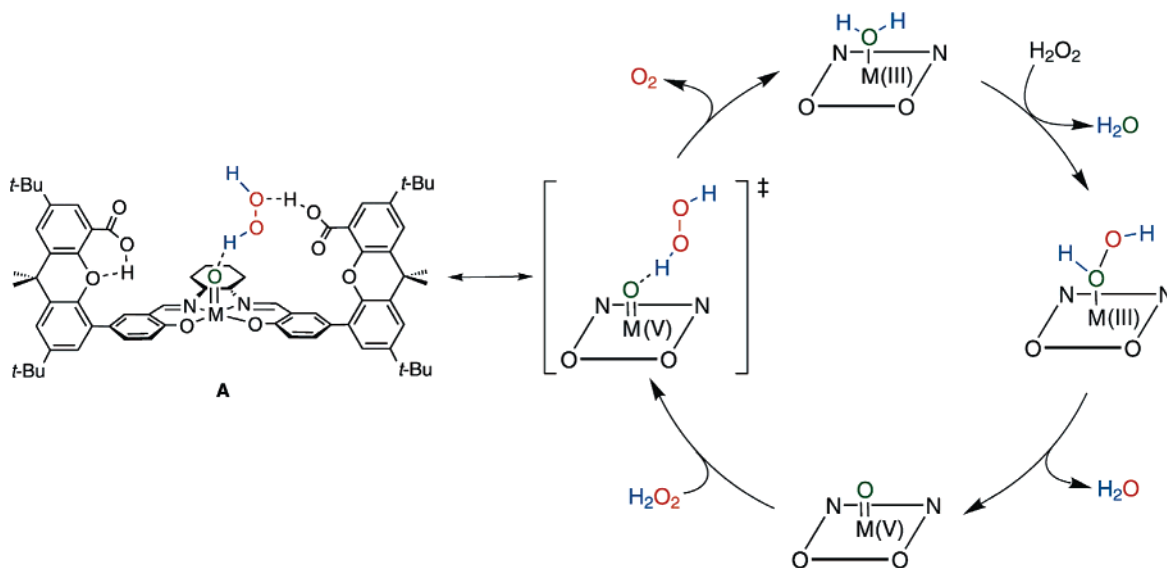
(17) Brooks, P. R.; Wirtz, M. C.; Vetelino, M. G.; Rescek, D. M.; Woodworth, G. F.; Morgan, B. P.; Coe, J. W. *J. Org. Chem.* **1999**, *64*, 9719–9712.

(18) Felix, A. M. *J. Org. Chem.* **1974**, *39*, 1427–1429.

(19) Ships, G., Jr.; Rebek, J., Jr. *Tetrahedron Lett.* **1994**, *35*, 6823–6825.

(20) Nicholls, P.; Fita, I.; Loewen, P. C. *Adv. Inorg. Chem.* **2001**, *51*, 51–106.

SCHEME 2



(benzoic acid) enhances the TON of the parent salen complex, but the activity remains far inferior to that of $\text{Mn}(\text{HSX}^*)\text{Cl}$ (**17**) and $\text{Mn}(\text{H}_{\text{ph}}\text{SX}^*)\text{Cl}$ (**19**), which manage the proton by intramolecular transfer from the hanging functional group. The superior activity of **17** and **19** is reflected in the activity profiles shown in Figure 2. Both **17** and **19** exhibit similar reactivity profiles. Initial turnover frequencies are similar for both catalysts, but **17** appears to be more robust over time and hence exhibits higher overall activity.

The role of the acid-to-metal distance in promoting catalase activity may be understood in the context of recent experimental and theoretical investigations of Mn–salen catalysts. The replacement of H_2O_2 by aryl peroxide permits the catalase cycle at a Hangman salen platform to be arrested, and accordingly, intermediates can be detected by stopped-flow spectroscopy.²¹ Proton transfer to the aryl peroxide coordinated to the Mn(III) center furnishes a high-valent Mn(V) oxo intermediate. The stopped-flow studies reveal that this step, however, is not rate-determining, and for this reason the acid-to-metal distance is less crucial for the first step in the catalase cycle in the Hangman systems. Instead, subsequent oxidation of peroxide by the Mn(V) oxo appears to be rate-determining, a contention that is supported by recent theoretical investigations of Mn salen catalase activity.^{22,23} The catalase cycle deduced from computational studies is shown in Scheme 2. The highest energy intermediate in the cycle (presumably giving rise to the rate-determining step) is found to be the Mn(V) oxo associated with H_2O_2 in an end-on fashion; this intermediate is depicted by A in Scheme 2 for the system reported here. The hanging acid–base group would be beneficial to promoting the formation of the end-on intermediate via a hydrogen-bonding network. Therefore, the $\{\text{Mn}(\text{V}) \text{oxo}-\text{H}_2\text{O}_2\}$ assembly is expected to be sensitive to the positioning of the acid–base group over the face of the salen platform. An energy-minimized calculation of the geometry of hydroperoxide-bound $\text{Mn}(\text{HSX}^*-\text{COOH})$ (with an ethylenediamine bridge instead of the cyclohexyl) demon-

strates the ligand can access a range of metal-to-acid distances depending on the rotation of the xanthene bridge around the macrocycle (Figure 3a). Whereas one carboxylic acid can hydrogen bond with the unbound oxygen on the hydroperoxide at an acid-to-metal distance of $\sim 5 \text{ \AA}$, the other forms an unconstructive intramolecular hydrogen bond with the oxygen on the xanthene. To form this intramolecular hydrogen bond, the xanthene tilts appreciably toward the plane of the macrocycle ring presumably driven by the stabilization incurred from the formation of the six-membered ring. This intramolecular bond has been observed in porphyrin xanthene complexes in the absence of substrate.²⁴ Hence, only one hanging group need be involved for substrate assembly, even when two are available. The hydrogen bond network is structurally different for the phenyl-spaced system. Two analogous energy-minimized calculation of the hydroperoxide-bound $\text{Mn}(\text{H}_{\text{ph}}\text{SX}^*-\text{COOH})$ (**19**) were performed. The first revealed that the addition of the phenylene spacer permits the two acids to comfortably span the distance above the salen platform to form an intramolecular carboxylic acid dimer (Figure 3b). An alternative structure was explored by tilting the xanthene scaffolds away from each other so that, while both carboxylic acids can still form productive hydrogen bonds with the bound hydroperoxide, they are not facing each other and thus cannot form a $-(\text{COOH})_2-$ dimer (Figure S3.1). The structure is destabilized by 44 kJ/mol relative to that of the $-(\text{COOH})_2-$ dimer (Table S3.2) showing that formation of the dimer confers significant stabilization to **19**. The formation of this stabilizing intramolecular hydrogen bond is likely accompanied by a decrease in the acidity of the proton over the reactive cleft. Accordingly, substrate assembly will be diminished due to the reduced ability to form additional hydrogen bonds, thus accounting for the lower catalase activity of **19** as compared to that of **17** (see Figure 1) where the two acids are too far apart to form an intramolecular dimer.

The modified chiral salen macrocycle transfers stereochemical information in an oxygen atom transfer reaction when H_2O_2 is replaced by prochiral substrates. With the use of sodium hypochlorite as the oxygen atom transfer source, epoxidation of the prochiral olefin 1,2-dihydronaphthalene by $\text{Mn}(\text{HSX}^*-\text{COOH})$ was investigated.

(21) Liu, S.-Y.; Soper, J. D.; Yang, J. Y.; Rybak-Akimova, E. V.; Nocera, D. G. *Inorg. Chem.*, **2006**, *45*, 7572–7574.

(22) Abashkin, Y. G.; Burt, S. K. *Inorg. Chem.* **2005**, *44*, 1425–1432.

(23) Abashkin, Y. G.; Burt, S. K. *J. Phys. Chem. B* **2004**, *108*, 2708–2711.

(24) Chang, C. K.; Bag, N.; Guo, B.; Peng, S.-M. *Inorg. Chim. Acta* **2003**, *351*, 261–268.

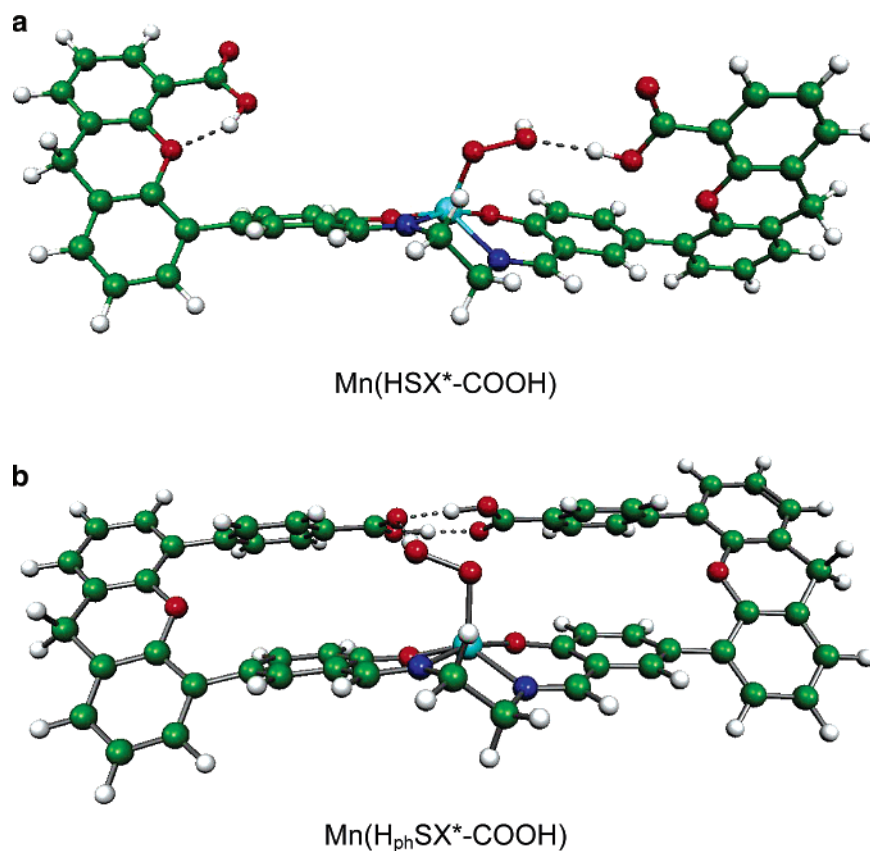


FIGURE 3. Energy-minimized structures obtained from DFT of the hydroperoxide complexes of (a) Mn(HSX*-COOH) showing one of the carboxylic acids is hydrogen bonded to the oxygen on the xantheno scaffold, while the other is hydrogen bonded to the hydroperoxide and (b) Mn(H_{ph}SX*-COOH) showing the two carboxylic acids span the face of the salen macrocycle to make a $-(\text{COOH})_2-$ dimer that interacts with the hydroperoxide via a hydrogen bond.

COOH)Cl (**17**) was examined. The epoxide product was resolved with 23% enantiomeric excess (ee), demonstrating communication with the chiral backbone and substrate despite the bulky xantheno functionalizations situated at the 5 and 5' position of the macrocycle. Whereas this ee is inferior to the best salen epoxidation catalysts, it is on par with the "introductory" ee's observed for first generation catalysts. More specifically, the ee is consistent with salen macrocycles unfunctionalized in the 3 and 3' positions.^{9,25,26} The addition of bulky functional groups in the 3 and 3' positions is believed to enhance the selectivity in epoxidation reactions by directing olefin approach over the chiral-inducing cyclohexyl bridge by sterically blocking alternative substrate orientations.^{10,25} With this in mind, we intend to modify the substituents about the macrocycle to optimize the enantiomeric selectivity of electron-rich substrates within this Hangman framework.

In conclusion, we have developed an easy and versatile methodology to install Hangman scaffolds on salen macrocycles while maintaining the ligand's chiral framework. Two functionalized xantheno scaffolds form a symmetric molecular cleft, which can be structurally tuned with spacers appended to the xantheno scaffold. Comparison of the reactivity profiles and overall TON for H₂O₂ dismutation between Hangman salens

with pendant acid and methyl ester groups establishes the importance of the hydrogen-bonding group in facilitating catalysis. Computational studies suggest that only one carboxylic acid is needed to promote the favored end-on hydrogen peroxide assembly with the metal oxo catalytic intermediate. When the functional group is extended with a phenylene spacer, the two carboxylic acids are sufficiently close to form a $-(\text{COOH})_2-$ dimer, which reduces the propensity of the hanging group to promote substrate assembly; accordingly, lower catalytic activity is observed. When the H₂O₂ substrate is replaced by prochiral substrates such as 1,2-dihydronaphthalene, asymmetric epoxidation is observed with introductory ee's of 23%. Increases in ee will be sought by introducing steric substituents at crucial positions on the salen macrocycle so as to promote substrate interaction with the chiral cyclohexyldiamine backbone of the salen macrocycle.

Experimental Section

General Information. Details are given in the Supporting Information.

4-(5-Bromo-2,7-di-*tert*-butyl-9,9-dimethyl-9H-xanthen-4-yl)-benzoic Acid (3**).** A solution of 4-(5-bromo-2,7-di-*tert*-butyl-9,9-dimethyl-9H-xanthen-4-yl)-benzoic acid methyl ester (**4**) (0.414 g, 0.773 mmol) in 10 mL of THF was refluxed with 5 mL of saturated sodium hydroxide in water for 2 h. The mixture was neutralized with aqueous HCl and extracted with 3 × 25 mL of dichloromethane. The combined organic layers were dried with MgSO₄, and the solvent was removed by rotary evaporation to yield the colorless product (0.334 g, 83.1% yield). ¹H NMR (500 MHz,

(25) Jacobsen, E. N.; Wu, M. H. In *Comprehensive Asymmetric Catalysis*; Jacobsen, E. N., Pfaltz, A., Yamamoto, H., Eds.; Springer: New York, 1999; pp 649–677.

(26) Lin, G.-Q.; Li, Y.-M.; Chan, A. S. C. In *Principles and Applications of Asymmetric Synthesis*; Wiley-Interscience: New York, 2001; pp 237–241.

CDCl_3 , δ): 8.07 (d, $J = 6.0$ Hz, 2H), 7.65 (d, $J = 6.0$ Hz, 2H), 7.48 (s, 1H), 7.36 (s, 1H), 7.30 (s, 1H), 7.22 (s, 1H), 1.63 (s, 6H), 1.28 (m, 18H). ^{13}C NMR (500 MHz, CDCl_3 , δ): 172.6, 147.1, 146.3, 145.5, 145.4, 144.0, 131.4, 130.6, 130.2, 130.1, 128.6, 128.3, 128.0, 126.3, 122.9, 121.8, 110.4, 35.6, 34.83, 34.79, 35.4, 31.7, 31.6. HRESI-MS ($[\text{M} + \text{H}]^+$) $\text{C}_{30}\text{H}_{33}\text{O}_3\text{Br}$ m/z , Calcd 521.1686, found 521.1679.

2,7-Di-*tert*-butyl-5-(3-formyl-4-methoxy-phenyl)-9,9-dimethyl-9H-xanthene-4-carboxylic Acid (5). Under nitrogen, a mixture of 4-hydroxycarbonyl-5-bromo-2,7-di-*tert*-butyl-9,9-dimethylxanthene (**1**) (0.150 g, 0.338 mmol), 3-formyl-4-methoxyphenylboronic acid (0.067 g, 0.371 mmol), sodium carbonate (0.052 g, 0.507 mmol), tetrakis(triphenylphosphine)palladium (0.015 g, 0.020 mmol), DMF (9 mL), and deionized water (1 mL) was heated to 90 °C for 36 h. Upon cooling, 10 mL of water was added, and the mixture was extracted with 3 × 25 mL of dichloromethane. The organic portions were combined and dried over MgSO_4 , and the solvent was removed by rotary evaporation. The crude solid was purified by column chromatography (silica gel, 8:2 pentane/ethyl acetate) to elute the colorless product (0.108 g, 64% yield). ^1H NMR (500 MHz, CDCl_3 , δ): 10.55 (s, 1H), 8.03 (d, $J = 2.5$ Hz, 1H), 7.98 (d, $J = 2.5$ Hz, 1H), 7.70 (dd, $J = 8.5$ Hz, 2 Hz, 1H), 7.68 (d, $J = 2.5$ Hz, 1H), 7.49 (d, $J = 2.5$ Hz, 1H), 7.21 (d, $J = 2$ Hz, 1H), 7.15 (d, $J = 8.5$ Hz, 1H), 4.02 (s, 3H), 1.73 (s, 6H), 1.37 (s, 9H), 1.34 (s, 9H). ^{13}C NMR (500 MHz, CDCl_3 , δ): 190.1, 167.8, 161.7, 148.3, 147.1, 146.3, 144.7, 137.6, 134.2, 131.3, 130.1, 130.0, 129.3, 128.21, 128.16, 126.4, 124.8, 122.1, 116.9, 112.2, 56.0, 35.1, 34.83, 34.80, 32.0, 31.7, 31.5. HRESI-MS ($[\text{M} - \text{H}]^-$) $\text{C}_{32}\text{H}_{35}\text{O}_5$ m/z , Calcd 499.2490, found 499.2482.

2,7-Di-*tert*-butyl-5-(3-formyl-4-methoxy-phenyl)-9,9-dimethyl-9H-xanthene-4-carboxylic Acid Methyl Ester (6). Under nitrogen, a mixture of 4-methoxycarbonyl-5-bromo-2,7-di-*tert*-butyl-9,9-dimethylxanthene (**2**) (0.300 g, 0.653 mmol), 3-formyl-4-methoxyphenylboronic acid (0.130 g, 0.722 mmol), sodium carbonate (0.101 g, 0.981 mmol), tetrakis(triphenylphosphine)palladium (0.029 g, 0.040 mmol), DMF (9 mL), and deionized water (1 mL) was heated to 90 °C for 36 h. Upon cooling, the mixture was extracted with 3 × 75 mL of dichloromethane. The organic portions were combined and dried over MgSO_4 , and the solvent was removed by rotary evaporation. The crude solid was purified by column chromatography (silica gel, 3:7 hexane/dichloromethane) to elute the colorless product (0.333 g, 99.1% yield). ^1H NMR (500 MHz, CDCl_3 , δ): 10.54 (s, 1H), 8.01 (d, $J = 2.5$ Hz, 1H), 7.85 (dd, $J = 8.5$ Hz, 2.5 Hz, 1H), 7.57 (s, 2H), 7.43 (d, $J = 2.5$ Hz, 1H), 7.21 (d, $J = 2.5$ Hz, 1H), 7.10 (d, $J = 8.5$ Hz, 1H), 4.01 (s, 3H), 3.50 (s, 3H), 1.70 (s, 6H), 1.36 (s, 9H), 1.33 (s, 9H). ^{13}C NMR (500 MHz, CDCl_3 , δ): 190.0, 167.7, 160.9, 147.4, 146.1, 145.3, 145.2, 138.2, 131.4, 131.1, 130.2, 130.0, 127.9, 126.3, 126.2, 125.9, 124.5, 121.9, 119.7, 111.2, 56.0, 52.0, 35.0, 34.7, 34.6, 32.1, 31.7, 31.5. HRESI-MS ($[\text{M} + \text{Na}]^+$) $\text{NaC}_{33}\text{H}_{38}\text{O}_5$ m/z , Calcd 537.2611, found 537.2601.

4-[2,7-Di-*tert*-butyl-5-(3-formyl-4-methoxy-phenyl)-9,9-dimethyl-9H-xanthene-4-yl]-benzoic Acid (7). Under nitrogen, a mixture of 4-(5-bromo-2,7-di-*tert*-butyl-9,9-dimethyl-9H-xanthene-4-yl)-benzoic acid (**3**) (0.300 g, 0.575 mmol), 3-formyl-4-methoxyphenylboronic acid (0.114 g, 0.633 mmol), sodium carbonate (0.089 g, 0.864 mmol), tetrakis(triphenylphosphine)palladium (0.025 g, 0.034 mmol), DMF (9 mL), and deionized water (1 mL) was heated to 90 °C for 36 h. Upon cooling, the mixture was extracted with 3 × 100 mL of dichloromethane. The organic portions were combined and dried over MgSO_4 , and the solvent was removed by rotary evaporation. The crude solid was purified by column chromatography (silica gel, 98:2 dichloromethane/methanol) to elute the colorless product (0.323 g, 97.3% yield). ^1H NMR (500 MHz, CDCl_3 , δ): 10.41 (s, 1H), 7.87 (s, 1H), 7.82 (s, 1H), 7.74 (d, $J = 1.25$ Hz, 1H), 7.49 (d, $J = 2.5$ Hz, 1H), 7.45 (d, $J = 2.5$ Hz, 1H), 7.43 (dd, $J = 6$ Hz, 2.5 Hz, 1H), 7.36 (d, $J = 8$ Hz, 2H), 7.18 (dd, $J = 8$ Hz, 2 Hz, 2H), 6.68 (d, $J = 8.5$ Hz, 1H), 3.96 (s, 3H), 1.75 (s, 6H), 1.37 (s, 9H), 1.36 (s, 9H). ^{13}C NMR (500 MHz, CDCl_3 ,

δ): 189.9, 171.9, 161.1, 146.0, 145.94, 145.88, 145.5, 137.4, 135.3, 130.9, 130.5, 130.0, 129.8, 129.7, 128.3, 128.2, 128.1, 127.0, 125.73, 125.70, 124.4, 122.7, 121.9, 111.0, 55.8, 35.4, 34.8, 31.83, 31.79, 31.77, 29.9, 27.5. HRESI-MS ($[\text{M} + \text{Na}]^+$) $\text{C}_{38}\text{H}_{40}\text{O}_5\text{Na}$ m/z , Calcd 599.2768, found 599.2757.

4-[2,7-Di-*tert*-butyl-5-(3-formyl-4-methoxy-phenyl)-9,9-dimethyl-9H-xanthene-4-yl]-benzoic Acid Methyl Ester (8). Under nitrogen, a mixture of 4-(5-bromo-2,7-di-*tert*-butyl-9,9-dimethyl-9H-xanthene-4-yl)-benzoic acid methyl ester (**4**) (0.200 g, 0.374 mmol), 3-formyl-4-methoxyphenylboronic acid (0.074 g, 0.411 mmol), sodium carbonate (0.058 g, 0.563 mmol), tetrakis(triphenylphosphine)palladium (0.016 g, 0.022 mmol), DMF (9 mL), and deionized water (1 mL) was heated to 90 °C for 36 h. Upon cooling, the mixture was extracted with 3 × 100 mL of dichloromethane. The organic portions were combined and dried over MgSO_4 , and the solvent was removed by rotary evaporation. The crude solid was purified by column chromatography (silica gel, dichloromethane) to elute the colorless product (0.219 g, 99.1% yield). ^1H NMR (500 MHz, CDCl_3 , δ): 10.39 (s, 1H), 7.77 (d, $J = 8.5$ Hz, 2H), 7.74 (d, $J = 2.5$ Hz, 1H), 7.47 (d, $J = 2.5$ Hz, 1H), 7.44 (d, $J = 2.5$ Hz, 1H), 7.38 (dd, $J = 8.5$ Hz, 2.5 Hz, 1H), 7.31 (d, $J = 8.5$ Hz, 2H), 7.16 (m, 2H), 6.57 (s, $J = 8.5$ Hz, 1H), 3.97 (s, 3H), 3.89 (s, 3H), 1.74 (s, 6H), 1.36 (s, 9H), 1.35 (s, 9H). ^{13}C NMR (500 MHz, CDCl_3 , δ): 190.3, 167.8, 161.5, 146.5, 146.42, 146.40, 146.3, 144.0, 138.1, 131.4, 131.3, 131.1, 130.4, 130.0, 129.7, 128.9, 128.5, 128.4, 126.23, 126.17, 124.9, 123.0, 122.4, 111.5, 56.2, 52.7, 35.9, 35.3, 32.3, 32.2. HRESI-MS ($[\text{M} + \text{Na}]^+$) $\text{C}_{39}\text{H}_{42}\text{O}_5\text{Na}$ m/z , Calcd 613.2924, found 613.2920.

2,7-Di-*tert*-butyl-5-(3-formyl-4-hydroxy-phenyl)-9,9-dimethyl-9H-xanthene-4-carboxylic Acid (9). 2,7-Di-*tert*-butyl-5-(3-formyl-4-methoxy-phenyl)-9,9-dimethyl-9H-xanthene-4-carboxylic acid (**5**) (0.545 g, 1.11 mmol) was added to 20 mL of dry dichloromethane, and the mixture was cooled to 0 °C. A solution of boron tribromide (3 mL, 1.0 M in dichloromethane) was added, and upon stirring for 3 h, 20 mL of water was added. The organic layer was separated, washed with 10 mL of water, and dried over MgSO_4 . The solvent was evaporated, and the residue was purified by column chromatography (silica gel, 98:2 dichloromethane/methanol) to elute the product (0.330 g, 62% yield). X-ray quality crystals were grown by slow evaporation of a saturated dichloromethane solution. ^1H NMR (500 MHz, CDCl_3 , δ): 11.13 (s, 1H), 9.97 (s, 1H), 8.02 (d, $J = 2.5$ Hz, 1H), 7.79 (d, $J = 2.5$ Hz, 1H), 7.71 (d, $J = 2.5$ Hz, 1H), 7.69 (d, $J = 2.5$ Hz, 1H), 7.50 (d, $J = 2.5$ Hz, 1H), 7.23 (d, $J = 2.5$ Hz, 1H), 7.13 (d, $J = 8.5$ Hz, 1H), 1.74 (s, 6H), 1.39 (s, 9H), 1.38 (s, 9H). ^{13}C NMR (500 MHz, CDCl_3 , δ): 198.0, 169.8, 160.8, 147.0, 146.4, 145.7, 145.3, 138.7, 136.0, 130.6, 130.4, 130.1, 127.5, 126.4, 125.9, 125.8, 122.2, 121.5, 120.5, 117.5, 44.9, 35.1, 34.8, 34.7, 32.2, 31.7, 31.6. HRESI-MS ($[\text{M} - \text{H}]^-$) $\text{C}_{31}\text{H}_{33}\text{O}_5$ m/z , Calcd 485.2323, found 485.2234.

2,7-Di-*tert*-butyl-5-(3-formyl-4-hydroxy-phenyl)-9,9-dimethyl-9H-xanthene-4-carboxylic Acid Methyl Ester (10). 2,7-Di-*tert*-butyl-5-(3-formyl-4-methoxy-phenyl)-9,9-dimethyl-9H-xanthene-4-carboxylic acid methyl ester (**6**) (0.200 g, 0.389 mmol) was added to 8 mL of dichloromethane, and the mixture was cooled to 0 °C. A solution of boron tribromide (1.2 mL, 1.0 M in dichloromethane) was added, and upon stirring for 1 h, 4 mL of water was added. The organic layer was separated, washed with 10 mL of water, and dried over MgSO_4 . The solvent was evaporated, and the residue was purified by column chromatography (silica gel, 99:1 dichloromethane/methanol) to elute the product (0.054 g, 28% yield). ^1H NMR (500 MHz, CDCl_3 , δ): 11.12 (s, 1H), 10.07 (s, 1H), 7.96 (d, $J = 2$ Hz, 1H), 7.76 (dd, $J = 8.5$ Hz, 2 Hz, 1H), 7.58 (d, $J = 2.5$ Hz, 1H), 7.56 (d, $J = 2$ Hz, 1H), 7.45 (d, $J = 2.5$ Hz, 1H), 7.25 (d, $J = 2$ Hz, 1H), 7.09 (d, $J = 8.5$ Hz, 1H), 3.55 (s, 3H), 1.71 (s, 6H), 1.38 (s, 9H), 1.34 (s, 9H). ^{13}C NMR (500 MHz, CDCl_3 , δ): 197.8, 167.5, 160.8, 147.3, 146.3, 145.4, 145.3, 138.9, 135.9, 131.0, 130.3, 130.2, 127.6, 126.4, 126.0, 125.8, 122.2, 120.3, 119.8, 117.2, 52.3, 35.1, 34.8, 34.7, 32.3, 31.8, 31.6. HRESI-MS ($[\text{M} + \text{H}]^+$) $\text{C}_{32}\text{H}_{37}\text{O}_5$ m/z , Calcd 501.2636, found 501.2625.

4-[2,7-Di-*tert*-butyl-5-(3-formyl-4-hydroxy-phenyl)-9,9-dimethyl-9H-xanthen-4-yl]-benzoic Acid (11). 4-[2,7-Di-*tert*-butyl-5-(3-formyl-4-methoxy-phenyl)-9,9-dimethyl-9H-xanthen-4-yl]-benzoic acid (**7**) (0.300 mg, 0.520 mmol) was added to 10 mL of dichloromethane, and the mixture was cooled to 0 °C. A solution of boron tribromide (1.6 mL, 1.0 M in dichloromethane) was added, and upon stirring for 2 h, 6 mL of water was added. The organic layer was separated, washed with 10 mL of water, and dried over MgSO₄. The solvent was evaporated, and the residue was purified by column chromatography (silica gel, 98:2 dichloromethane/methanol) to elute the product (0.181 g, 62% yield). ¹H NMR (500 MHz, C₄D₈O, δ): 9.45 (s, 1H), 7.74 (d, *J* = 8 Hz, 1H), 7.68 (d, *J* = 8 Hz, 1H), 7.54 (d, *J* = 2 Hz, 2H), 7.45 (m, 4H), 7.31 (d, *J* = 8 Hz, 1H), 7.23 (dd, *J* = 10.5, 1.5 Hz, 1H), 6.73 (d, *J* = 8.5 Hz, 1H), 1.36 (s, 18H). ¹³C NMR (500 MHz, C₄D₈O, δ): 196.9, 167.5, 161.7, 146.74, 146.66, 143.6, 138.6, 135.5, 133.0, 132.9, 132.5, 131.6, 131.5, 130.7, 130.6, 130.3, 130.1, 129.4, 129.3, 129.0, 126.7, 126.5, 123.3, 122.8, 121.8, 117.7, 36.1, 35.4, 32.0, 25.8, 25.6, 25.3, 25.2. HRESI-MS ([M - H]⁻) C₃₇H₃₇O₅ *m/z*, Calcd 561.2646, found 561.2646.

4-[2,7-Di-*tert*-butyl-5-(3-formyl-4-hydroxy-phenyl)-9,9-dimethyl-9H-xanthen-4-yl]-benzoic Acid Methyl Ester (12). 4-[2,7-Di-*tert*-butyl-5-(3-formyl-4-methoxy-phenyl)-9,9-dimethyl-9H-xanthen-4-yl]-benzoic acid methyl ester (**8**) (0.100 g, 0.169 mmol) was added to 8 mL of dichloromethane, and the mixture was cooled to 0 °C. A solution of boron tribromide (0.51 mL, 1.0 M in dichloromethane) was added, and upon stirring for 1 h, 4 mL of water was added. The organic layer was separated, washed with 10 mL of water, and dried over MgSO₄. The solvent was evaporated, and the residue was purified by column chromatography (silica gel, dichloromethane) to elute the product (0.076 g, 78% yield). ¹H NMR (500 MHz, CDCl₃, δ): 10.87 (s, 1H), 9.29 (s, 1H), 7.26 (d, *J* = 8.5 Hz, 2H), 7.49 (d, *J* = 2.5 Hz, 1H), 7.46 (m, 2H), 7.33 (m, 2H), 7.31 (s, 1H), 7.20 (d, *J* = 2 Hz, 1H), 7.17 (d, *J* = 2 Hz, 1H), 6.85 (d, *J* = 8.5 Hz, 1H), 4.00 (s, 3H), 1.76 (s, 6H), 1.37 (s, 18H). ¹³C NMR (500 MHz, CDCl₃, δ): 197.0, 167.4, 161.1, 146.5, 146.4, 146.1, 146.0, 143.6, 138.6, 135.8, 130.93, 130.91, 130.4, 130.3, 129.6, 129.1, 128.9, 128.1, 126.3, 126.0, 123.2, 122.7, 120.8, 117.8, 52.8, 35.8, 35.3, 32.7, 32.3. HRESI-MS ([M + Na]⁺) C₃₈H₄₀O₅Na *m/z*, Calcd 599.2768, found 599.2756.

H₂(HSX*–COOH) (13). 2,7-Di-*tert*-butyl-5-(3-formyl-4-hydroxy-phenyl)-9,9-dimethyl-9H-xanthen-4-carboxylic acid (**9**) (0.100 g, 0.206 mmol) was combined with (1*R*,2*R*)-(–)-1,2-diaminocyclohexane (0.012 g, 0.103 mmol) in 4 mL of absolute ethanol, and the mixture was refluxed for 12 h. Upon cooling, the solvent was removed by rotary evaporation, and the resulting yellow solid was washed with 1 mL of cold methanol and dried under vacuum to yield 0.100 g of product (92% yield). ¹H NMR (500 MHz, CDCl₃, δ): 8.63 (s, 2H), 7.90 (d, *J* = 2 Hz, 2H), 7.76 (d, *J* = 2.5 Hz, 2H), 7.58 (d, *J* = 2.5 Hz, 2H), 7.38 (m, 4H), 7.23 (d, *J* = 2 Hz, 2H), 6.95 (d, *J* = 8.5 Hz, 2H), 3.60 (d, *J* = 9.5 Hz, 2H), 2.07 (d, *J* = 11.5 Hz, 2H), 1.95 (d, *J* = 9.5 Hz), 1.76 (s, 6H), 1.73 (m, 2H), 1.68 (s, 2H), 1.61 (s, 6H), 1.36 (s, 18H), 1.35 (s, 18H). HRESI-MS ([M - H]⁻) C₆₈H₇₇N₂O₈ *m/z*, Calcd 1049.5676, found 1049.5676.

H₂(HSX*–COOMe) (14). 2,7-Di-*tert*-butyl-5-(3-formyl-4-hydroxy-phenyl)-9,9-dimethyl-9H-xanthen-4-carboxylic acid methyl ester (**10**) (0.050 g, 0.100 mmol) was combined with (1*R*,2*R*)-(–)-1,2-diaminocyclohexane (0.006 mg, 0.050 mmol) in 5 mL of absolute ethanol, and the mixture was refluxed for 8 h. Upon cooling, the solvent was removed by rotary evaporation, and the resulting solid was washed with 1 mL of cold methanol and dried under vacuum to yield the product as a yellow solid (0.053 g, 98%). ¹H NMR (500 MHz, CDCl₃, δ): 13.42 (bs, 2H), 8.46 (s, 2H), 7.55 (d, *J* = 2.5 Hz, 2H), 7.52 (d, *J* = 2.5 Hz, 2H), 7.56 (s, 2H), 7.45 (d, *J* = 2.5 Hz, 2H), 7.38 (d, *J* = 2.5 Hz, 2H), 7.16 (d, *J* = 2.5 Hz, 2H), 6.96 (d, *J* = 9 Hz, 2H), 3.45 (d, *J* = 9 Hz, 2H), 3.32 (s, 6H), 1.99 (d, *J* = 9 Hz, 2H), 1.92 (d, *J* = 9 Hz, 2H), 1.78 (d, *J* = 9 Hz, 2H), 1.69 (s, 6H), 1.67 (s, 6H), 1.53 (t, *J* = 9 Hz, 2H), 1.43 (s,

9H), 1.33 (s, 9H). ¹³C NMR (500 MHz, CDCl₃, δ): 168.2, 165.3, 160.3, 147.4, 146.0, 145.4, 145.2, 134.0, 133.2, 131.2, 130.1, 129.1, 128.6, 126.2, 126.1, 125.7, 121.4, 120.1, 118.3, 116.5, 72.9, 52.1, 35.1, 34.73, 34.70, 33.5, 32.1, 31.9, 31.7, 31.6, 24.4. HRESI-MS ([M + H]⁺) C₇₀H₈₃N₂O₈ *m/z*, Calcd 1079.6144, found 1079.6167.

H₂(H_{ph}SX*–COOH) (15). 4-[2,7-Di-*tert*-butyl-5-(3-formyl-4-hydroxy-phenyl)-9,9-dimethyl-9H-xanthen-4-yl]-benzoic acid (**11**) (0.025 g, 0.044 mmol) was combined with (1*R*,2*R*)-(–)-1,2-diaminocyclohexane (0.003 g, 0.022 mmol) in 5 mL of absolute ethanol, and the mixture was refluxed for 15 h. Upon cooling, the solvent was removed by rotary evaporation, and the resulting yellow solid was washed with 0.5 mL of cold methanol and dried under vacuum to yield the product as a dull yellow solid (0.026 g, 97% yield). ¹H NMR (500 MHz, CDCl₃, 25 °C, δ): 7.91 (m, 4H), 7.47 (d, *J* = 7 Hz, 2H), 7.68 (m, 4H), 7.55 (d, *J* = 7 Hz, 2H), 7.39 (m, 4H), 7.19 (m, 2H), 7.11 (s, 2H), 7.10 (s, 2H), 3.54 (bs, 2H), 2.33 (bs, 4H), 2.05 (bs, 4H), 1.72 (s, 12H), 1.35 (s, 18H), 1.30 (s, 18H). HRESI-MS ([M - H]⁻) C₈₀H₈₅N₂O₈ *m/z*, Calcd 1201.6311, found 1201.6329.

H₂(H_{ph}SX*–COOMe) (16). 4-[2,7-Di-*tert*-butyl-5-(3-formyl-4-hydroxy-phenyl)-9,9-dimethyl-9H-xanthen-4-yl]-benzoic acid methyl ester (**12**) (0.018 g, 0.031 mmol) was combined with (1*R*,2*R*)-(–)-1,2-diaminocyclohexane (0.002 g, 0.016 mmol) in 5 mL of absolute ethanol, and the mixture was refluxed for 8 h. Upon cooling, the solvent was removed by rotary evaporation, and the resulting yellow solid was washed with 0.5 mL of cold methanol and dried under vacuum (0.019 mg, 98% yield). ¹H NMR (500 MHz, CDCl₃, δ): 13.09 (bs, 2H), 8.05 (s, 2H), 7.65 (d, *J* = 8 Hz, 2H), 7.61 (d, *J* = 8 Hz, 2H), 7.43 (d, *J* = 1.5 Hz, 2H), 7.35 (d, *J* = 2 Hz, 2H), 7.20 (m, 4H), 7.13 (d, *J* = 2 Hz, 2H), 7.09 (d, *J* = 1.5 Hz, 2H), 7.02 (m, 4H), 6.50 (d, *J* = 8 Hz, 2H), 4.37 (t, *J* = 11.5 Hz, 2H), 3.25 (bs, 2H), 2.97 (m, 4H), 1.72 (s, 6H), 1.67 (s, 6H), 1.53 (bs, 2H), 1.34 (s, 18H), 1.38 (s, 18H). ¹³C NMR (500 MHz, CDCl₃, δ): 167.1, 164.8, 160.3, 146.1, 145.9, 145.6, 142.9, 138.1, 135.3, 133.5, 132.8, 130.9, 130.43, 130.37, 129.6, 129.0, 128.8, 128.5, 128.1, 125.8, 125.6, 122.2, 121.2, 118.2, 116.3, 72.8, 52.1, 35.4, 34.8, 34.74, 34.68, 33.0, 32.14, 32.11, 31.7, 31.2, 29.91, 29.87, 29.6, 24.4. HRESI-MS ([M + H]⁺) C₈₂H₉₁N₂O₈ *m/z*, Calcd 1231.6770, found 1231.6799.

Mn(HSX*–COOH)Cl (17). H₂(HSX*–COOH) (**13**) (0.100 g, 0.095 mmol) and manganese(II) acetate tetrahydrate (0.035 g, 0.143 mmol) were added to 8 mL of ethanol, and the mixture was refluxed for 3 h in air. Upon cooling, 1 mL of an aqueous saturated sodium chloride solution was added, and after stirring for 5 min, an additional 10 mL of water was added. The mixture was then extracted with 2 × 6 mL of dichloromethane. The combined organic portions were then washed with 5 mL of water and dried over MgSO₄. The solvent was removed by rotary evaporation to yield the brown product (0.101 g, 93% yield). HRESI-MS ([M - Cl]⁻) C₆₈H₇₆MnN₂O₈ *m/z*, Calcd 1103.4977, found 1103.4931. Anal. Calcd for C₆₈H₇₆ClMnN₂O₈·2H₂O: C, 69.46; H, 6.86; N, 2.38. Found: C, 69.65; H, 6.67; N, 2.21.

Mn(HSX*–COOMe)Cl (18). H₂(HSX*–COOMe) (**14**) (0.020 g, 0.019 mmol) and manganese(II) acetate tetrahydrate (0.007 g, 0.029 mmol) were added to 4 mL of ethanol, and the mixture was refluxed for 2 h in air. Upon cooling, 0.5 mL of an aqueous saturated sodium chloride solution was added, and the mixture was extracted with 2 × 15 mL of dichloromethane. The combined organic portions were then washed with 15 mL of water and dried over MgSO₄. The solvent was removed by rotary evaporation to yield the brown product (0.021 g, 98% yield). HRESI-MS ([M - Cl]⁻) C₇₀H₈₀MnN₂O₈ *m/z*, Calcd 1131.5290, found 1131.5318. Anal. Calcd for C₇₀H₈₀ClMnN₂O₈: C, 72.00; H, 6.90; N, 2.40. Found: C, 71.82; H, 6.72; N, 2.48.

Mn(H_{ph}SX*–COOH)Cl (19). H₂(H_{ph}SX*–COOH) (**15**) (0.010 g, 0.008 mmol) and manganese(II) acetate tetrahydrate (0.003 g, 0.012 mmol) were added to 3 mL of ethanol, and the mixture was refluxed for 4 h in air. Upon cooling, 0.5 mL of an aqueous saturated sodium chloride solution was added, and the mixture was

extracted with 2 × 15 mL of dichloromethane. The combined organic portions were then washed with 15 mL of water and dried over MgSO₄. The solvent was removed by rotary evaporation to yield the brown product (0.010 g, 93% yield). HRESI-MS ([M – Cl][−]) C₈₀H₈₄MnN₂O₈ *m/z*, Calcd 1255.5603, found 1255.5605. Anal. Calcd for C₈₀H₈₄ClMnN₂O₈: C, 74.37; H, 6.55; N, 2.17. Found: C, 74.21; H, 6.72; N, 2.10.

Mn(H_{ph}SX*–COOMe)Cl (20), H₂(H_{ph}SX*–COOMe) (**16**) (0.010 g, 0.008 mmol) and manganese(II) acetate tetrahydrate (0.003 g, 0.012 mmol) were added to 3 mL of ethanol, and the mixture was refluxed for 4 h in air. Upon cooling, 0.5 mL of an aqueous saturated sodium chloride solution was added, and the mixture was extracted with 2 × 15 mL of dichloromethane. The combined organic portions were then washed with 15 mL of water and dried over MgSO₄. The solvent was removed by rotary evaporation to yield the brown product (0.010 g, 93% yield). HRESI-MS ([M – Cl][−]) C₈₂H₈₈MnN₂O₈ *m/z*, Calcd 1283.5926, found 1283.5857. Anal. Calcd for C₈₂H₈₈ClMnN₂O₈: C, 74.61; H, 6.72; N, 2.12. Found: C, 74.53; H, 6.60; N, 2.10.

(R,R)-N,N'-Bis(5-phenylsalicylidene)-1,2-cyclohexanediamine (22). 4-Hydroxy-biphenyl-3-carbaldehyde (**21**) (0.300 g, 1.51 mmol) was refluxed with (1R,2R)-(–)-1,2-diaminocyclohexane (0.086 g, 0.757 mmol) in 5 mL of absolute ethanol for 12 h, and the mixture was then cooled to 0 °C and filtered. The precipitate was collected by vacuum filtration and washed with 2 × 5 mL of cold ethanol and dried in vacuo to yield 0.241 g of the bright yellow product in 67% yield. ¹H NMR (500 MHz, CDCl₃, δ): 13.39 (bs, 2H), 8.35 (s, 2H), 7.50 (d, *J* = 2 Hz, 2H), 7.47 (m, 2H), 7.46 (s, 2H), 7.40 (s, 2H), 7.38 (m, 4H), 7.30 (s, 2H), 7.29 (s, 2H), 6.97 (d, *J* = 9 Hz, 2H), 3.38 (d, *J* = 9 Hz, 2H), 1.99 (m, 2H), 1.92 (d, *J* = 9 Hz, 2H), 1.78 (d, *J* = 9 Hz, 2H), 1.51 (t, *J* = 9 Hz, 2H). ¹³C NMR (500 MHz, CDCl₃, δ): 165.0, 160.7, 140.4, 132.1, 131.2, 130.1, 128.9, 126.9, 126.7, 118.9, 117.5, 72.9, 33.3, 24.3. HRESI-MS ([M + H]⁺) C₃₂H₃₁N₂O₂ *m/z*, Calcd 475.2380, found 475.2371.

Mn[(R,R)-N,N'-Bis(5-phenylsalicylidene)-1,2-cyclohexanediaminato]Cl (23). (R,R)-N,N'-Bis(5-phenylsalicylidene)-1,2-cyclohexanediamine (**22**) (0.050 g, 0.105 mmol) and manganese(II) acetate tetrahydrate (0.039 g, 0.158 mmol) were added to 4 mL of ethanol, and the mixture was refluxed for 4 h in air. Upon cooling, 1 mL of an aqueous saturated sodium chloride solution was added, and the mixture was extracted with 2 × 15 mL of dichloromethane. The combined organic portions were then washed with 15 mL of water and dried over MgSO₄. The solvent was removed by rotary evaporation to yield a brown product (0.050 g, 84% yield). HRESI-MS ([M – Cl][−]) C₃₂H₂₈MnN₂O₂ *m/z*, Calcd 527.1526, found 527.1518. Anal. Calcd for C₃₂H₂₈ClMnN₂O₂: C, 68.27; H, 5.01; N, 4.98. Found: C, 68.20; H, 5.21; N, 5.08.

5-(Boronic Acid)-2,7-di-tert-butyl-9,9-dimethyl-9H-xanthene-4-carboxylic Acid Methyl Ester (24). Under nitrogen, 4-methoxycarbonyl-5-bromo-2,7-di-tert-butyl-9,9-dimethylxanthene (**2**) (1.00 g, 2.18 mmol), bis(pinacolato)diboron (0.830 g, 3.27 mmol), potassium acetate (0.747 g, 7.63 mmol), and dichloro[1,1'-bis(diphenylphosphino)ferrocene]palladium(II) dichloromethane adduct (0.159 g, 0.218 mmol) were added to 10 mL of anhydrous dimethyl sulfoxide, and the mixture was heated to 90 °C for 36 h. Upon cooling, 60 mL of benzene was added, and the solution was washed with 3 × 100 mL of deionized water. The organic layer was dried over MgSO₄ and reduced by rotary evaporation to obtain a black crude product which was taken up in 200 mL of hexane and filtered; this was repeated three times. The combined filtrates were reduced by rotary evaporation, and the resulting solid was recrystallized in hot isopropyl alcohol to yield the product as a white crystalline solid upon cooling (0.398 g, 43% yield). X-ray quality crystals were grown from isopropyl alcohol. ¹H NMR (500 MHz, CDCl₃, δ): 7.56 (d, *J* = 2.5 Hz, 1H), 7.51 (d, *J* = 2.5 Hz, 1H), 7.48 (m, 2H), 3.95 (s, 3H), 1.62 (s, 6H), 1.41 (bs, 2H), 1.34 (s, 9H), 1.33 (s, 9H). ¹³C NMR (500 MHz, CDCl₃, δ): 166.7, 152.6, 149.1, 145.8, 145.0, 135.5, 131.4, 128.6, 128.0, 127.4, 126.2, 125.5, 116.2, 64.3, 52.8,

34.5, 33.0, 32.9, 31.7, 31.5, 24.9. HRESI-MS ([M + H]⁺) C₂₅H₃₄O₅B *m/z*, Calcd 425.2495, found 425.2494.

5-Bromo-2,7-di-tert-butyl-9,9-dimethyl-9H-xanthene-4-carboxylic Acid Benzyl Ester (25). 4-Hydroxycarbonyl-5-bromo-2,7-di-tert-butyl-9,9-dimethylxanthene (**1**) (0.500 g, 1.12 mmol), 4-(dimethylamino)pyridine (0.013 g, 0.107 mmol), and benzyl alcohol (0.12 mL, 1.12 mmol) were added to 50 mL of dry dichloromethane, and the solution was cooled to 0 °C in an ice water bath. To this, 1.22 mL of a 1.0 M solution of 3-dicyclohexylcarbodiimide in dichloromethane (1.22 mmol) was added, and the reaction mixture was stirred at 0 °C for 10 min, then warmed to room temperature. Upon stirring for an addition 6 h at room temperature, the solution was again cooled to 0 °C, filtered, and washed with a minimal amount of cold dichloromethane (about 6 mL). The filtrate was reduced by rotary evaporation; the crude product was purified by column chromatography (silica gel, 9:1 hexane/ethyl acetate) to elute the product as a pale yellow oil that solidified under vacuum overnight (0.599 g, 99% yield). ¹H NMR (500 MHz, CDCl₃, δ): 7.71 (d, *J* = 2.5 Hz, 1H), 7.54 (m, 3H), 7.45 (d, *J* = 2.4 Hz, 1H), 7.38 (m, 2H), 7.33 (m, 2H), 5.50 (s, 2H), 1.65 (s, 6H), 1.34 (s, 9H), 1.33 (s, 9H). ¹³C NMR (500 MHz, CDCl₃, δ): 167.1, 147.4, 147.3, 145.7, 145.3, 136.5, 131.1, 130.7, 128.74, 128.72, 128.68, 128.3, 126.7, 126.6, 121.7, 119.7, 110.5, 67.3, 35.4, 34.79, 34.76, 32.2, 31.6, 20.8. HRESI-MS ([M + Na]⁺) C₃₁H₃₅O₅BrNa *m/z*, Calcd 557.16406, found 557.1641.

2,7-Di-tert-butyl-5-(3-formyl-4-hydroxy-phenyl)-9,9-dimethyl-9H-xanthene-4-carboxylic Acid Benzyl Ester (26). Under nitrogen, 5-bromo-2,7-di-tert-butyl-9,9-dimethyl-9H-xanthene-4-carboxylic acid benzyl ester (**25**) (0.500 g, 0.93 mmol), potassium acetate (0.321 g, 3.27 mmol), bis(pinacolato)diboron (0.355 g, 1.40 mmol), and dichloro[1,1'-bis(diphenyl-phosphino)ferrocene]palladium (II) dichloromethane adduct (0.068 g, 0.093 mmol) were added to 5 mL of anhydrous dimethyl sulfoxide, and the mixture was heated to 90 °C for 24 h. Upon cooling, 25 mL of benzene was added, and the solution was washed with 3 × 50 mL of water and dried with MgSO₄. The solvent was removed by rotary evaporation, and the resulting crude black oil was put under vacuum overnight to give a crude black solid. The solid was stirred in 100 mL of hexane and filtered; this procedure was repeated three times. The combined filtrate was rotary evaporated to reveal a semicrystalline colorless solid which was used without further purification. (The ¹H NMR showed this to be the desired intermediate 2,7-di-tert-butyl-9,9-dimethyl-5-(4,4,5,5-tetramethyl-[1,3,2]dioxaborolan-2-yl)-9H-xanthene-4-carboxylic acid benzyl ester along with some 2,3-dimethyl-butane-2,3-diol impurities from hydrolysis of the bis-(pinacolato)diboron.) Under nitrogen, this was added to 5-bromosalicylaldehyde (0.187 g, 0.93 mmol), sodium carbonate (0.144 g, 1.39 mmol), dichloro[1,1'-bis(diphenylphosphino)ferrocene]palladium (II) dichloromethane adduct (0.041 g, 0.056 mmol), 14 mL of 1,2-dimethoxyethane, and 6 mL of deionized water, and the mixture was heated to 90 °C for 48 h. Upon cooling, 50 mL of dichloromethane was added, and the solution was washed with 2 × 50 mL of deionized water. The combined aqueous layers were extracted with 20 mL of dichloromethane, and the combined organic layers were dried with MgSO₄. Upon solvent removal by rotary evaporation the crude solid was purified by column chromatography (silica gel, 8:2 hexane/ethyl acetate) to elute the desired product as a colorless solid (0.100 g, 19%). ¹H NMR (500 MHz, CDCl₃, δ): 11.03 (s, 1H), 9.96 (s, 1H), 7.91 (d, *J* = 2.5 Hz, 1H), 7.72 (dd, *J* = 8.5 Hz, 2 Hz, 1H), 7.58 (m, 2H), 7.46 (d, *J* = 2 Hz, 1H), 7.24 (m, 4H), 7.15 (m, 2H), 7.00 (2, *J* = 8.5 Hz, 1H), 5.06 (s, 2H), 1.71 (s, 6H), 1.37 (s, 9H), 1.33 (s, 9H). HRESI-MS ([M + Na]⁺) C₃₈H₄₀O₅Na *m/z*, Calcd 599.2768, found 599.2781.

2,7-Di-tert-butyl-5-(3-formyl-4-hydroxy-phenyl)-9,9-dimethyl-9H-xanthene-4-carboxylic Acid Methyl Ester (10) via (24). Under nitrogen, 2,7-di-tert-butyl-5-(3-formyl-4-hydroxy-phenyl)-9,9-dimethyl-9H-xanthene-4-carboxylic acid methyl ester (**10**) (0.250 g, 0.590 mmol), 5-bromosalicylaldehyde (0.119 g, 0.590 mmol), sodium carbonate (0.092 g, 0.884 mmol), dichloro[1,1'-bis(diphe-

nylphosphino)ferrocene]palladium(II) dichloromethane adduct (0.026 g, 0.035 mmol), 14 mL of dimethoxyethane, and 6 mL of deionized water were heated to 90 °C for 48 h. Upon cooling, 25 mL of dichloromethane was added, and the solution was washed with 2 × 25 mL of deionized water. The aqueous portions were extracted with 10 mL of dichloromethane. The combined organic portions were dried under MgSO₄, and the solvent was removed by rotary evaporation; the resulting residue was purified by column chromatography (silica gel, 99:1 dichloromethane/methanol) to elute the product as a colorless solid (0.118 g, 40% yield).

2,7-Di-*tert*-butyl-5-(3-formyl-4-hydroxy-phenyl)-9,9-dimethyl-9H-xanthen-4-carboxylic Acid (9) via Deprotection of (10). 2,7-Di-*tert*-butyl-5-(3-formyl-4-hydroxy-phenyl)-9,9-dimethyl-9H-xanthen-4-carboxylic acid methyl ester (10) (0.050 g, 0.10 mmol) was added to 8 mL of dichloromethane, and the mixture was cooled to 0 °C. A solution of boron tribromide (1.2 mL, 1.0 M in dichloromethane) was added, and the reaction mixture was warmed to room temperature and stirred for 4 h, after which 4 mL of water was added. The organic layer was separated, washed with 10 mL of water, and dried over MgSO₄. The solvent was evaporated, and the residue was purified by column chromatography (silica gel, 99:5 dichloromethane/methanol) to elute the product (0.014 g, 28% yield).

2,7-Di-*tert*-butyl-5-(3-formyl-4-hydroxy-phenyl)-9,9-dimethyl-9H-xanthen-4-carboxylic Acid (9) via Deprotection of (26). Under nitrogen, 2,7-di-*tert*-butyl-5-(3-formyl-4-hydroxy-phenyl)-9,9-dimethyl-9H-xanthen-4-carboxylic acid benzyl ester (26) (0.100 g, 0.174 mmol) was added to 20 mL of ethyl acetate and palladium (5% on activated carbon, 0.015 g), and the mixture was placed under a hydrogen balloon overnight at room temperature. The mixture was then filtered over Celite, the filtrate was reduced by rotary evaporation, and the residue was purified by column chromatography (silica gel, 95:5 dichloromethane/methanol) to elute the desired product 26 (0.061 g, 72%) yield.

Hydrogen Peroxide Disproportionation Reactions. Dismutation reactions were performed at room temperature in a sealed (PTFE septum) 20 mL reaction vial equipped with a magnetic stirbar and a capillary gas delivery tube linked to an inverted graduated buret filled with water. The reaction vial was charged with a stock solution of the corresponding catalyst in CH₂Cl₂ (1.0 mL). Methanol (0.5 mL) was added, followed by H₂O₂ (790 μL, 8.22 mmol; 10.4 M (30%) aq solution), and the reaction mixture was stirred vigorously. The time was set to zero immediately after addition of H₂O₂. The conversion was monitored volumetrically, and the amount of produced O₂ (*n*) was calculated through the perfect gas equation $pV = nRT$, assuming that $p = 1$ atm. As a check on our experimental setup, MnO₂ was employed to dismutate the hydrogen peroxide completely. Calibration runs show that the amount of oxygen collected matches the amount expected, given the concentration of the hydrogen peroxide solution.

The amount of catalyst used to obtain the results of Figures 1 and 2 was as follows: Mn(5-phsalen)Cl (23) (1.0 mL from a solution of 5.3 mg in 10 mL of CH₂Cl₂ or 0.00095 mmol) to give an average of 1.01 mL of O₂ in 1 h. Mn(5-phsalen)Cl (23) with 1 equiv of benzoic acid (1.0 mL from a solution of 2.7 mg of Mn(5-phsalen)Cl and 0.6 mg of benzoic acid in 5 mL of CH₂Cl₂ or 0.00095 mmol of each) to give 3.21 mL of O₂ in 1 h. Mn(HSX*–COOH)Cl (17) (1.0 mL from a solution of 5.6 mg in 5 mL of CH₂Cl₂ or 0.00095 mmol) to give 35.91 mL of O₂ in 1 h. Mn(HSX*–COOMe)Cl (18) (1.0 mL from a solution of 5.54 mg in 5 mL of CH₂Cl₂ or 0.00095 mmol) to give 1.61 mL of O₂ in 1 h. Mn(H_{ph}–SX*–COOH)Cl (19) (1.0 mL from a solution of 2.5 mg in 2 mL of CH₂Cl₂ or 0.00095 mmol) to give 18.01 mL of O₂ in 1 h. Mn(H_{ph}–SX*–COOMe)Cl (20) (1.0 mL from a solution of 2.5 mg in 2 mL of CH₂Cl₂ or 0.00095 mmol) to give 2.01 mL of O₂ in 1 h. The standard deviations on the TON measurements over 1 h are derived from at least three data points.

Epoxidation of 1,2-Dihydronaphthalene. The epoxidation method and conditions are modified from previous epoxidation studies using manganese salen complexes.²⁷ A volume of 1 mL of a 0.05 M solution of Na₂HPO₄ was added to 2.5 mL of commercial bleach. The pH of this solution (~55 M in NaOCl) was adjusted to pH 11 by the dropwise addition of 1.0 M NaOH solution, and the mixture was cooled to 0 °C. This was added to a precooled 0 °C solution of 1,2-dihydronaphthalene (100 mg, 0.77 mmol) and Mn(HSX*–COOH) (17) (85 mg, 0.077 mmol, 10% catalyst loading) in 2 mL of dichloromethane. Upon stirring for 12 h, the layers were separated, and the aqueous layer was extracted with 2 × 6 mL of dichloromethane. The combined organic layers were washed with 10 mL of water and 10 mL of a saturated sodium chloride solution and dried over MgSO₄. After solvent removal by rotary evaporation the crude product was purified to by column chromatography (silica gel, 98:2 petane/ethyl acetate) to yield the epoxide product (0.090 g, 83% yield).

DFT Calculations. Gas-phase density functional theoretical (DFT) calculations of Mn(HSX*–COOH) and Mn(H_{ph}SX*–COOH) were performed using the Amsterdam Density Functional (ADF2002.02)^{28,29} package on a home-built Linux cluster of 60 Intel processors running in parallel groups of 12. To simplify the calculation, the *tert*-butyl and methyl groups were removed from the xanthenes, as well as replacing the cyclohexyl backbone to ethylenediamine. The generalized gradient approximation (GGA) was implemented by use of Becke's 1988 exchange functional³⁰ and Perdew et al.'s 1991 correlation functional.³¹ The basis set was of triple- ζ quality for manganese, oxygen, and nitrogen, with a double set of polarization functions for Mn and a single polarization set for O and N, and of double- ζ quality with a single polarization set for C and H; the frozen core approximation was used for the 1s shell of C, N, and O and for the 1s, 2s, and 2p shells of Mn. Full geometry optimizations of the entire complexes were run at 0 K. All computations were carried out in the quintet spin state, and the spin restriction was lifted. The molecular geometries and the spatial components of the resulting Kohn–Sham single-electron wave functions were visualized and analyzed using the software Molekel.^{32,33}

Acknowledgment. We thank Professor Timothy Jamison for the use of his chiral gas chromatograph, Chudi Ndubaku and Ryan Moslin for instrument assistance, David R. Manke for assistance in obtaining and solving the X-ray crystal structures, the MIT Department of Chemistry Instrumentation Facility for performing high-resolution mass spectroscopy, and Shih-Yuan Liu, Steve Reece, Leng Leng Chng, and Christopher J. Chang for fruitful discussions. This work was supported by funding from the DOE DE-FG02-05ER15745.

Supporting Information Available: Initial synthetic scheme, X-ray crystal structures and related tables, ¹H NMR spectra of selected compounds, selected bond distances from the DFT calculations of the Hangman compounds, as well as general experimental methods. This material is available free of charge via the Internet at <http://pubs.acs.org>.

JO0613075

(27) Zheng, W.; Jacobsen, E. N. *J. Org. Chem.* **1991**, *56*, 2296–2298.
(28) te Velde, G.; Bickelhaupt, F. M.; van Gisbergen, A. J. A.; Fonseca Guerra, C.; Baerends, E. J.; Snijders, J. G.; Ziegler, T. *J. Comput. Chem.* **2001**, *22*, 931–967.

(29) Fonseca Guerra, C.; Snijders, J. G.; te Velde, G.; Baerends, E. J. *Theor. Chem. Acc.* **1998**, *99*, 391–403.

(30) Becke, A. D. *Phys. Rev. A* **1998**, *38*, 3098–3100.

(31) Perdew, J. P.; Chevary, J. A.; Vosko, S. H.; Jackson, K. A.; Pederson, M. R.; Singh, D. J.; Fiolhais, C. *Phys. Rev. B* **1992**, *46*, 6671–6687.

(32) Flükiger, P.; Lüthi, H. P.; Portmann, S.; Weber, J. *Molekel*, version 4.2/3; Swiss Center for Scientific Computing: Manno, Switzerland, 2000–2002.

(33) Portmann, S.; Lüthi, H. P. *Chimica* **2000**, *54*, 776–780.